

# Statistical Inverse Lighting

Eduardo Fernández<sup>1</sup> and Gonzalo Besuievsky<sup>2</sup>

<sup>1</sup>*Centro de Cálculo, Universidad de la República, Montevideo, Uruguay*

<sup>2</sup>*Geometry and Graphics Group, Universitat de Girona, Girona, Spain*

Keywords: Inverse Lighting, Radiosity.

Abstract: Inverse lighting techniques allows to obtain the unknown light sources parameters, such as light position or flux emission, from desired lighting intentions. In this paper we present a new inverse lighting technique that uses the statistical mean and variance of the illuminated scene to obtain optimal solutions for a given lighting intention. This technique allows to explore a huge number of full radiosity solutions in a short time, reducing in this way drastically the optimization time required.

## 1 INTRODUCTION

Lighting intentions (LI) are the goals that designers would like to achieve in the illumination design process. Given an interior space to illuminate, this process achieves several steps that goes from the use of the space to the specific light accentuation to be obtained (Russell, 2008). Once the LIs are specified the designer provides the set of parameters that must fulfill the intentions. Then, the light positions, shape and power of the emitters, must be selected.

The management of all lighting parameters is a huge combinatorial problem. Usually, to find a solution, the problem is treated as an inverse method. That is, a method where the illumination aspects are unknown and must be determined. The whole process involves two main computational tasks: the global illumination simulation and the search of an optimal solution. The first one is crucial to obtain accurate lighting information. For the second one, an optimization process is used to fulfill the requirements.

Most of the previous work on inverse lighting for global illumination problems provides good numerical methods, omitting timing considerations, which can be a problem for interactive design.

In this paper we present a new inverse lighting method, that focus on the use of statistical LI and that greatly improves timing of previous work. Our main contribution is to introduce a new technique that relates LIs to the lighting mean and variance of the scene. Our method exploits coherence of interior spaces to build a compact radiosity representation that is efficiently used to quickly explore many

lighting solutions. We present previous work is in Section 2 and the background for lighting representation we used in Section 3. Our statistical approach is introduced in Section 4 and test results are shown in Section 5. Finally, conclusions and future work are summarized in Section 6.

## 2 PREVIOUS WORK

One of the first attempts to infer emitter positions and shapes given lighting intentions, is presented in (Schoeneman et al., 1993) through the intuitive principle of "Painting with light", but where the interactivity is achieved only for direct illumination. In our work we are focusing on indirect illumination.

In the context of radiosity, several works driven by different motivations and assumptions were proposed. A survey on all these methods can be found in (Patow and Pueyo, 2003). In (Contensin, 2002), an Inverse Radiosity method based on a pseudo-inverse of the radiosity matrix is formulated. Kawai et al. (Kawai et al., 1993) perform the optimization over the intensities and directions of a set of lights, as well as surface reflectivity, in order to best convey the subjective impression of certain scene qualities expressed by users. In (Castro et al., 2012), an heuristic search algorithm combined with linear programming is used to optimize light positioning with an energy-saving goal.

In all inverse lighting methods the coherence is used to improve the global illumination computation. In (Castro et al., 2012), a re-using random walk paths technique is employed. They store an irradiance ma-

trix that allows computing, for each patch of the scene the power contribution of fixed light points. We based our work on the low-rank radiosity method (LRR) (Fernández, 2009), that allows to obtain a full radiosity solution in real time with changing lighting parameters and small computer storage.

Our work deals also with optimization problems. These problems consists of finding the best solution from all of the feasible solutions, which are defined through a set of constraints. For illumination purposes, each constraint is related to a lighting intention for all or part of the scene. To find an optimal solution, heuristic approach are used, which avoid visiting the whole search space. There are a large number of heuristic search algorithms in the literature, which can potentially be used to solve lighting problems (hill climbing, beam search and simulated annealing) (Russell and Norvig, 2003). In (Castro et al., 2012) a wide range of these algorithms are explored. In (Cassol et al., 2011) and (Schneider et al., 2009), the scenes are simplified to rectangular spaces, and the inverse problem is solved through a generalized extremal optimization approach. In (Fernández and Besuievsky, 2012), the Variable Neighborhood Search (VNS) method (Hansen and Mladenovic, 2001) was used. We also used VNS for the present work.

### 3 COMPACT LIGHTING REPRESENTATION

Lighting intentions (LI) are defined as goals that designers must provide to achieve the desired illumination. Designers can set many LI. Examples of LIs are: "Guarantee a minimum of irradiance in a panel in order to be seen correctly" or "Distribute the light homogeneously over all surfaces" (Figure 1).

In the discrete radiosity problem, the radiosity of the scene is computed by solving the linear system shown in Eq. 1 (Cohen et al., 1993).

$$(\mathbf{I} - \mathbf{RF})L_B = E \quad (1)$$

where  $\mathbf{I}$  is the identity matrix with dimension  $n \times n$  ( $n$  is the number of patches),  $\mathbf{R}$  is a diagonal matrix that stores the reflectivity of the patches,  $\mathbf{F}$  is the form factors matrix,  $L_B$  is a vector with the radiosity values, and  $E$  is the emission vector. The designer goal is to find  $E$  (to configure the position and radiosity values of the light sources), so that  $L_B$  meets all LI.

Usually the  $\mathbf{F}$  matrix is not computed, due to memory constraints. The  $n \times n$  matrix  $\mathbf{M}$  of Eq. 2 also has high order of complexity, so is rarely computed.

$$L_B = \mathbf{ME} \quad (2)$$

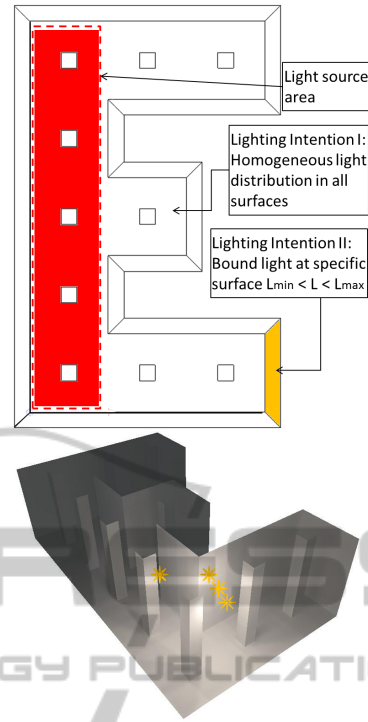


Figure 1: A top-view scene with a lighting intention configuration example (top) and a possible solution for positioning four light sources (bottom).

In this paper we use information from the  $\mathbf{M}$  matrix to define LIs, for this purpose, so we use the low-rank radiosity (LRR) methodology (Fernández, 2009). In LRR the matrix  $\mathbf{F}$  is approximated by the product of two matrices ( $\mathbf{UV}^T$ ), with dimension  $n \times k$  ( $n \gg k$ ). The  $O(nk)$  memory needed, allows storing  $\mathbf{U}$  and  $\mathbf{V}^T$  in the main memory. This work also exposes an approximation of the  $\mathbf{M}$  matrix (see Eq. 3) introducing  $\mathbf{Y}$ , which is also a  $n \times k$  matrix.

$$L_B = \mathbf{ME} \sim (\mathbf{I} - \mathbf{YV}^T)E \quad (3)$$

where  $\mathbf{Y} = -\mathbf{RU}(\mathbf{I} - \mathbf{V}^T\mathbf{RU})^{-1}$

### 4 STATISTICAL BASED LI

In statistics (Canavos, 1984), the mean ( $\mu$ ) and the standard deviation ( $\sigma$ ) are used to describe properties about sets of numerical data.  $\mu$  describes the central tendency of the data and  $\sigma$  measures their dispersion. In this paper is used  $\mu$  and  $\sigma$  to describe LIs. We show that  $\mu(L_B(\mathbf{s}))$  and  $\sigma(L_B(\mathbf{s}))$  could be obtained without the previous calculation of  $L_B(p)$  for patches  $p$  belonging to the scene  $\mathbf{s}$ . Here we explain the calculation process of  $\mu$  and  $\sigma$ , and how can be used in LI.

#### 4.1 Mean ( $\mu$ ) of $L_B(\mathbf{s})$

Radiosity is defined as light flux per unit of surface, so it is the mean (weighted by the area of the patches) of the flux density on all patches (Eq. 4).

$$\begin{aligned} \mu(L_B(\mathbf{s}, E)) &= \sum_{p \in \mathbf{s}} \mathbf{W}_A(i, i) L_B(p, E) = \\ &= (\mathbf{1}_s^T \mathbf{W}_A \mathbf{M}) E = V_{L_B}(\mathbf{s}) \cdot E \end{aligned} \quad (4)$$

In Eq. 4,  $\mathbf{W}_A$  is a diagonal matrix with weights ( $\mathbf{W}_A(i, i) = A(i, i) / \sum_j A(j, j)$ ).  $V_{L_B}(\mathbf{s})$  is a  $n \times 1$  vector.

In the calculation of the radiosity on a static scene the vector  $V_{L_B}(\mathbf{s})$  does not varies. In summary,  $\mu(L_B(\mathbf{s}))$  can be computed with complexity  $O(n)$ , using a single dot product.

#### 4.2 Standard Deviation ( $\sigma$ ) of $L_B(\mathbf{s})$

The standard deviation ( $\sigma$ ) is a scale parameter which determines the dispersion of a data set. Any radiosity vector can be interpreted as a list of sample data of a “random variable  $L_B$ ” which varies on a surface. Figure 2 shows an E-shaped scene with five different configurations of lights. Each  $L_B$  has its own  $\sigma(L_B)$  value, which measures the dispersion of the radiosity values along each scene. The more homogeneously illuminated the scene, the lower  $\sigma(L_B)$  associated, because of the small dispersion of the  $L_B$  lighting values.

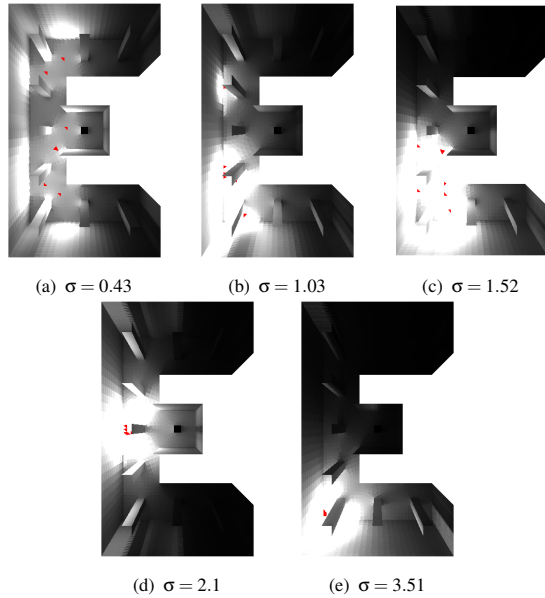


Figure 2: Different radiosity distributions in the “E” scene ( $n=24736$ ), and their  $\sigma$  values. Red patches are the emitters.

To speed up the calculation of  $\sigma(L_B)$ , we consider  $L_B$  as a linear combination of random variables: the vector  $L_B$  can be defined as a linear combination of

the  $\mathbf{M}$  columns (Eq. 5):

$$L_B = \mathbf{M}E = \sum_i \mathbf{M}(:, i) E(i) \quad (5)$$

where  $\mathbf{M}(:, i)$  is the sample data of an  $i^{\text{th}}$  random variable. Also is important the relation between the variance and the covariances, as expressed in Eq. 6.

$$\text{var}\left(\sum_i L_i a_i\right) = \sum_{ij} \text{cov}(L_i, L_j) a_i a_j, \quad (6)$$

In Eq. 6,  $L_i$  and  $L_j$  are random variables,  $a_i$  and  $a_j$  are constants, and  $\text{cov}$  is the covariance between  $L_i$  and  $L_j$ . Then, Eqs. 5 and 6 can be combined as:

$$\text{var}(L_B) = \text{var}\left(\sum_i \mathbf{M}(:, i) E(i)\right) =$$

$$\sum_{ij} \text{cov}(\mathbf{M}(:, i), \mathbf{M}(:, j)) E(i) E(j) = E^T \text{cov}(\mathbf{M}) E \quad (7)$$

In equation Eq. 7,  $\text{cov}(\mathbf{M})$  is a  $n \times n$  covariance matrix, where each element  $\text{cov}(\mathbf{M})(i, j)$  is the covariance associated with the  $i^{\text{th}}$  and  $j^{\text{th}}$  variables of  $\mathbf{M}$  (with sample data  $\mathbf{M}(:, i)$  and  $\mathbf{M}(:, j)$ ).

#### 4.3 Low-rank Covariance Matrix

In Eq. 7,  $\text{cov}(\mathbf{M})$  concentrates all geometric information, so, when the geometry is static it can be calculated in a precomputation stage. But an important drawback of this equation is the  $O(n^2)$  memory needed to store  $\text{cov}(\mathbf{M})$ . Fortunately, because of the lighting coherence in the scenes, the correlation between lighting data of close patches is high, so the  $\text{cov}(\mathbf{M})$  is a numerically low-rank matrix. Figure 3 shows the covariance matrix and its singular value decomposition (SVD) of a Cornell box. It can be appreciated that  $\text{cov}(\mathbf{M})$  has many pairs of similar rows. The plot of the SVD values (Figure 3 (b)) confirms that it is composed with redundant information.

To build a smaller covariance matrix, we replace the matrix  $\mathbf{M}$  in Eq. 7 by its low-rank variant  $\mathbf{YV}^T$  (Eq. 3) producing a  $k \times k$  covariance matrix (Eq. 8).

$$\begin{aligned} \text{var}(L_B) &\sim \text{var}(\mathbf{YV}^T E) = \\ \text{var}\left(\sum_i \mathbf{Y}(:, i) (\mathbf{V}^T E)_i\right) &= (\mathbf{V}^T E)^T \text{cov}(\mathbf{Y}) (\mathbf{V}^T E) \end{aligned} \quad (8)$$

In this equation  $(\mathbf{V}^T E)$  is  $k \times 1$  and  $(\mathbf{V}^T E)_i$  is the  $i^{\text{th}}$  element. Also, each column  $\mathbf{Y}(:, i)$  contains the sample values of a random variable. Finally,  $\text{cov}(\mathbf{Y})$  is the  $k \times k$  covariance matrix associated to those variables.

A brute force calculation of  $\text{var}(L_B)$  using Eq. 8 consumes  $O(nk)$  operations. This result is higher than the complexity obtained for  $\mu$  calculation. As stated in (Fernández et al., 2012), for any scene with coarse and fine-grained meshes, it is possible to build a sparse

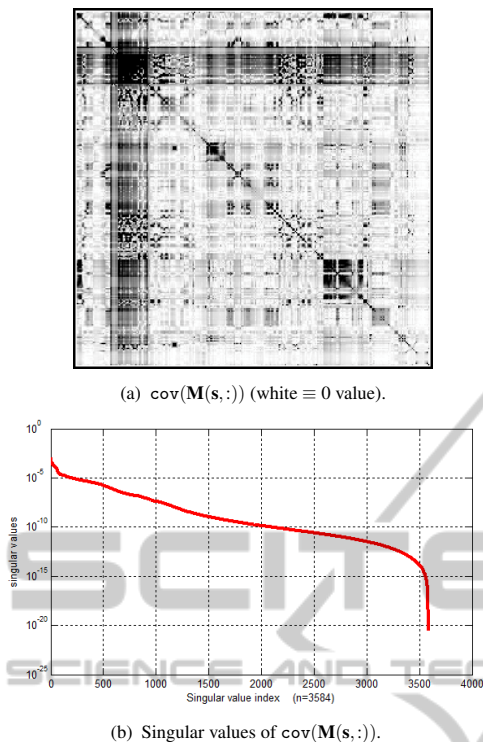


Figure 3: Covariance matrix and its SVD decomposition for a Cornell box with 3584 patches.

matrix  $\mathbf{V}$  such that the complexity of  $\mathbf{V}^T \mathbf{E}$  product could be reduced to  $O(n)$ . So, through a careful use of Eq. 8, the complexity of the variance can be reduced to  $O(n + e^2)$  where  $e$  is the number of emitter patches in the coarse-grained mesh.

#### 4.4 Chebyshev's based Constraints

A designer may want to optimize the lighting scene using certain LI, wishing to minimize the consumption of artificial light, but also bounding the light levels or the contrast. All these LI can be transformed into optimization goals and constraints, using  $\mu$  and  $\sigma$  parameters. For instance, to control a given constraint to be fulfilled ( $L_{min} \leq L_B(p) \forall p \in \mathbf{s}$ ), we have to calculate all the  $L_B(p)$  values, which has complexity  $O(nk)$ . A  $O(n)$  option consists in finding  $\mu(L_B(\mathbf{s}))$  and  $\sigma(L_B(\mathbf{s}))$  to bound the probability of any  $p$  to fulfill the constraint. The inequation 9 shows a new constraint formulation, where the parameter  $a$  establishes the probability of success in the transformation.

$$L_{min} \leq \mu(L_B(\mathbf{s})) - a\sigma(L_B(\mathbf{s})) \quad (9)$$

To explain the meaning of  $a$ , we base our reasoning in the Chebyshev's inequality (Canavos, 1984):

$$P[a\sigma(L_B(\mathbf{s})) \leq |\mu(L_B(\mathbf{s})) - L_B(p)|] \leq \frac{1}{a^2}, \forall p \in \mathbf{s}$$

where  $P$  is the probability function. This inequality is fulfilled for any  $L_B$  independently of their distribution. It can be demonstrated that when the new constraint is fulfilled, the probability of failure in the original constraint is  $\frac{1}{a^2}$  (Inequation 10).

$$P[L_B(p) \leq L_{min}] \leq \frac{1}{a^2} \quad (10)$$

This result is a probabilistic approach, and as such, does not guarantee certainty whatsoever. The new constraint built is a worst case boundary, meaning that smaller values of  $a$  also can provide good results.

## 5 TEST RESULTS

We built three experiments for solving inverse lighting problems. For the first one we aim to demonstrate the use of the variance as a LI. In the second one, we analyze the method changing statistical parameters for optimization. Those experiments have an average time execution of 10s for each run, and each experiment is carried out 20 times, totalizing 200s. Finally, a performance comparison of the proposed method with other methods is evaluated. All simulations were performed in a Matlab environment on a notebook computer (Intel Core i7-2670QM 2.2 Ghz processor with Turbo Boost up to 3.1 Ghz and 4 GB DDR3 memory).

Our optimization engine is based on the Variable Neighborhood Search (VNS) method (Hansen and Mladenovic, 2001). VNS is a single-solution based metaheuristic that finds global optimum solutions. However, we believe that similar results could be achieved with another optimization engine.

### 5.1 Dispersion

In this experiment we show the use of  $\sigma$  to manage the distribution of the light in the scene.

**Scene:** "E" corridor ( $\mathbf{s}_{Ec}$ ). ( $n \times k$ )=(24736  $\times$  1546).

**Goal:** We seek to illuminate the scene in a uniform manner, positioning six diffuse light sources.

**LI Goal Translation:**  $\min \sigma(L_B(\mathbf{s}_{Ec}))$ .

**Constraints Translation:** i) Six emitters. ii) Emitters are located in the installation area  $e$  (the red-colored rectangle in Figure 1). iii) The radiosity value of emitters is unique and predefined.

**Variables:** 12. Six 2D coordinates that delimit the location of the light sources.

**Running Details:** i) The precomputation of  $\mathbf{Y}$ ,  $\mathbf{V}$ , and  $\text{cov}(\mathbf{Y})$ , to apply the Eq. 8, takes about 12

minutes. ii) The VNS algorithm is executed 20 times. iii) 25000 evaluations of  $\sigma$  on each run, totaling half a million evaluations.

**Results:** i) Min, max, and mean of the  $\sigma$  values found: 0.425, 0.442, and 0.430. ii) Sample image: Figure 2 (a). Figures 2 (b), (c), and (d) were found adding to this experiment a constraint ( $\sigma \geq k$ ), and changing the value of  $k$  for each image. Figure 2 (e) was found changing the goal to  $\max \sigma(L_{Br}(\mathbf{s}))$ .

## 5.2 Statistical Tools for LI

In this experiment we analyze the convenience of using  $\mu$  and  $\sigma$  to satisfy a wide variety of LI. The experiment is developed on the same scene and with the same implementation than the previous one. Four different LI aspects were tested on a specific wall of the scene (the “yellow-colored wall” in Figure 1).

### ⊕ Illuminate

**Goal:** to illuminate the wall as much as possible, positioning six diffuse light sources.

**LI Goal Translation :**  $\max \mu(L_B(s_{Y_w}))$ .

**Results:** Min, max, and mean of the  $\mu$  values found: 0.394, 0.427, and 0.420. See Figure 4 (a).

### ⊕ Overshadow

**Goal:** to overshadow the wall as much as possible.

**LI Goal Translation:**  $\min \mu(L_B(s_{Y_w}))$ .

**Results:** Min, max, mean of  $\mu$  values:  $7.2 \times 10^{-4}$ ,  $7.64 \times 10^{-4}$ ,  $7.38 \times 10^{-4}$ . See Figure 4 (b).

### ⊕ Disseminate

**Goal:** to disseminate homogeneously the light over the wall, within radiosity boundaries.

**LI Goal Translation:**  $\min \sigma(L_B(s_{Y_w}))$ .

**LI Constraint Translation:**  $.30 \leq \mu(L_B) \leq .35$ .

**Results:** Min, max, and mean of the  $\sigma$  values found: 0.066, 0.073, and 0.067. See Figure 4 (c).

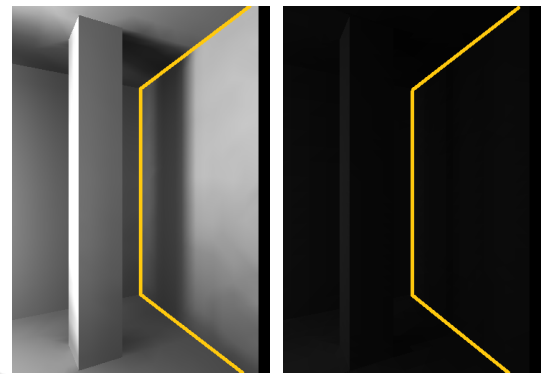
### ⊕ Contrast

**Goal:** the highest contrast illumination as possible in the wall, within radiosity boundaries.

**LI Goal Translation:**  $\max \sigma(L_B(\mathbf{s}))$ .

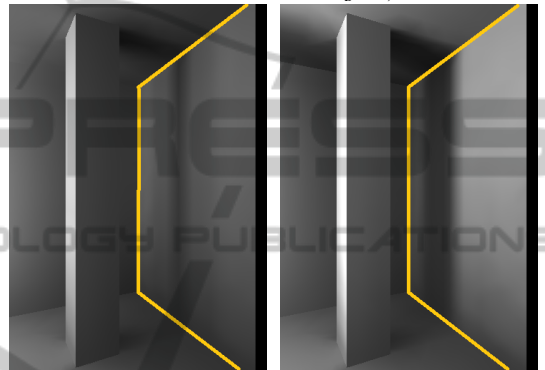
**LI Constraint Translation:**  $.30 \leq \mu(L_B) \leq .35$ .

**Results:** Min, max, and mean of the  $\sigma$  values found: 0.159, 0.175, and 0.171. See Figure 4 (d).



(a)  $\max \mu(=.442)$

(b)  $\min \mu(=7e-4)$  (the image shows  $L_B \times 50$ )



(c)  $\min \sigma(=.066)$  subject to  $.30 \leq \mu(L_B) \leq .35$

(d)  $\max \sigma(=.175)$  subject to  $.30 \leq \mu(L_B) \leq .35$

Figure 4: Four LI configurations applied to the “yellow-colored wall” (see Figure 1).

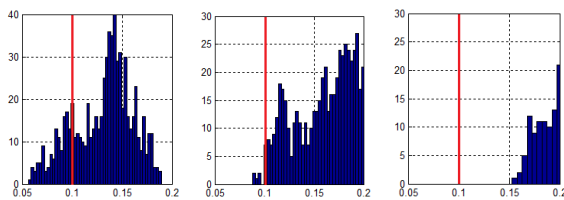
## 5.3 Chebyshev-based Constraints

In this experiment we test the new constraint built (see Ineq. 9), minimizing  $\mu(L_B(p))$  and replacing  $L_{min}=0.1 \leq L_B(p)$ ,  $\forall p \in$  “colored-yellow wall” with  $L_{min}=0.1 \leq \mu(L_B(\mathbf{s})) - a\sigma(L_B(\mathbf{s}))$ .

Three values were tested for the parameter  $a$ : 1, 2, and 3 (see Figures 5 (a), (b), and (c)). According to Chebyshev,  $a = 3$  means that less than 1/9 of all patches have values below 0.1, but the test shows a better result, because no patch is below the boundary.

## 5.4 Performance Comparison

The statistical inverse lighting method (SIL) allows to evaluate half a million  $\mu$  and  $\sigma$  in less than four minutes. This result greatly improves previous work. We compare this result performing the same test with two different inverse lighting approaches, as used in (Fernández and Besuievsky, 2012): using the full LRR method and using LRR but computing only the radiosity at the wall (LRR+) (see Table 1).



(a)  $.1 \leq \mu - \sigma$ . ( $\mu=.13$ ,  $\sigma=.026$ ). (b)  $.1 \leq \mu - 2\sigma$ . ( $\mu=.17$ ,  $\sigma=.034$ ). (c)  $.1 \leq \mu - 3\sigma$ . ( $\mu=.30$ ,  $\sigma=.063$ ).

Figure 5: The LI ( $\min \mu(L_B(s))$  subject to  $.1 \leq L_B$ ) is modeled with three values of  $a$  (from left to right:  $a=1, 2$ , and  $3$ ).

Table 1: Comparative of optimization approaches against our statistical technique.

| Method | Tests/s | Total time (min) | Speed-Up |
|--------|---------|------------------|----------|
| SIL    | 2083    | 4                | -        |
| LRR+   | 59      | 141              | 35       |
| LRR    | 8       | 1041             | 260      |

## 6 CONCLUSIONS AND FUTURE WORK

In this paper is presented a new methodology for achieving LI for inverse lighting problems. Our approach is based on the use of  $\mu$  and  $\sigma$  as statistical parameters for the lighting values. Using a low-rank formulation, we demonstrate that  $\mu$  and  $\sigma$  for  $L_B$  can be computed in  $O(n)$  and  $O(n + e^2)$ . This result allows to perform thousands of global illumination evaluation on a desktop PC, reducing drastically the overall optimization time required. We believe that this technique could open a new avenue in the search for optimal inverse lighting solutions. The results shown could lead to the use of the method in more complex scenes with more elaborated lighting intentions. Related to further development, more effort should be focus on an automatic parametrization of the LI.

## ACKNOWLEDGEMENTS

This work was partially funded by Programa de Desarrollo de las Ciencias Básicas (Uruguay) and by grant TIN2010-20590-C02-02 from Ministerio de Ciencia e Innovación (Spain).

## REFERENCES

- Canavos, G. (1984). *Applied probability and statistical methods*. Little, Brown.
- Cassol, F., Schneider, P. S., França, F. H., and Neto, A. J. S. (2011). Multi-objective optimization as a new approach to illumination design of interior spaces. *Building and Environment*, 46(2):331 – 338.
- Castro, F., del Acebo, E., and Sbert, M. (2012). Energy-saving light positioning using heuristic search. *Engineering Applications of Artificial Intelligence*, 25(3):566 – 582.
- Cohen, M., Wallace, J., and Hanrahan, P. (1993). *Radiosity and realistic image synthesis*. Academic Press Professional, Inc., San Diego, CA, USA.
- Contensin, M. (2002). Inverse lighting problem in radiosity. *Inverse Problems in Engineering*, 10(2):131–152.
- Fernández, E. (2009). Low-rank radiosity. In Rodríguez, O., Serón, F., Joan-Arinyo, R., and J. Madeiras, J. Rodríguez, E. C., editors, *Proceedings of the IV Iberoamerican Symposium in Computer Graphics*, pages 55–62. Sociedad Venezolana de Computación Gráfica, DJ Editores, C.A.
- Fernández, E. and Besuievsky, G. (2012). Inverse lighting design for interior buildings integrating natural and artificial sources. *Computers & Graphics*, 36(8):1096–1108.
- Fernández, E., Ezzatti, P., Nesmachnow, S., and Besuievsky, G. (2012). Low-rank radiosity using sparse matrices. In *Proceedings of GRAPP2012*, pages 260–267.
- Hansen, P. and Mladenovic, N. (2001). Variable neighborhood search: Principles and applications. *European Journal of Operational Research*, 130(3):449–467.
- Kawai, J. K., Painter, J. S., and Cohen, M. F. (1993). Radioptimization - goal based rendering. In *ACM SIGGRAPH 93*, pages 147–154, Anaheim, CA.
- Patow, G. and Pueyo, X. (2003). A survey of inverse rendering problems. *Computer Graphics Forum*, 22(4):663–688.
- Russell, S. (2008). *The Architecture of Light: Architectural Lighting Design, Concepts and Techniques: a Textbook of Procedures and Practices for the Architect, Interior Designer and Lighting Designer*. Conceptnine.
- Russell, S. J. and Norvig, P. (2003). *Artificial Intelligence: A Modern Approach*. Pearson Education, 2 edition.
- Schneider, P. S., Mossi, A. C., Franca, F. H. R., de Sousa, F. L., and da Silva Neto, A. J. (2009). Application of inverse analysis to illumination design. *Inverse Problems in Science and Engineering*, 17(6):737–753.
- Schoeneman, C., Dorsey, J., Smits, B., Arvo, J., and Greenberg, D. (1993). Painting with light. In *Proceedings of the 20th annual conference on Computer graphics and interactive techniques*, ACM SIGGRAPH 93, pages 143–146, New York, NY, USA. ACM.